

# Comparative Studies of Work-developing Capacity of Shape Memory Alloys (SMA) and Polymers

DIANA LACATUSU<sup>1\*</sup>, MIHAELA BAICAN<sup>1</sup>, FLORINA CRIVOI<sup>1</sup>, ALINA MONICA MIFTODE<sup>2</sup>

<sup>1</sup> Grigore T. Popa University of Medicine and Pharmacy Iasi, Faculty of Pharmacy, Physics Department, 16 Universitatii Str., 700115 Iasi, Romania

<sup>2</sup> Grigore T. Popa University of Medicine and Pharmacy Iasi, Faculty of Pharmacy, Department of Inorganic Chemistry, 16 Universitatii Str., 700115 Iasi, Romania

*The thermodynamic and work-generating behaviours of a Cu-14.86 Zn-5.81 Al (mass. %) shape memory alloy (SMA) and a three-layer PET heat shrinkable sheath were comparatively discussed. The experimental CuZnAl SMA under study experienced a reversible martensitic transformation and was able to lift over 4.8 mm, during heating-cooling cycles, a load which was 463 times heavier than the specimen. During heating, the PET fragments underwent up to three glass transitions and the PET ring-shaped specimens were able to lift over 3 mm, a load which was 1571 times heavier. By comparing the work generating capacity of CuZnAl SMA and PET heat shrinkable sheath, defined as the ratio between total absorbed enthalpy and specific work output, it was found out that the former has been ten times less effective than the latter.*

*Keywords: shape memory alloy, heat-shrinkable sheath, work-generating shape memory effect, martensitic transformation, glass transition.*

Recent progresses in material sciences and physics lead to the implementation of the term “phase change materials” (PCM) which, with the advent and maturation of micro-system technology, encompasses a great variety of materials undergoing Solid/Liquid, Solid/Gas, Solid/Solid, Liquid/Gas, Mesomorphic/Isotropic, Sol/Gel and Glass transitions [1]. Among these categories, the materials undergoing a Solid/Solid transition represent a promising class of “stimulus responsive materials” causing reduced environmental impact and high energy coupling efficiency [2]. One of the most common stimuli, that can trigger Solid/Solid transitions, is temperature and some of the most popular examples of solid state phase transitions are martensitic transformation and glass transition.

The former is diffusionless and occurs in shape memory alloys (SMAs) while the latter is diffusion controlled and occurs in shape memory polymers (SMPs) [3, 4]. Although SMAs and SMPs are driven by different types of transformations, the present paper aims to comparatively emphasize the thermodynamic and macroscopic changes governing their shape memory behaviour.

Firstly, the crystalline structures of both CuZnAl SMAs and polyethylene terephthalate (PET) have long period stacking order along 0z axis. In CuZnAl SMAs martensitic transformation changes the B2 cubic structure of  $\beta_2$  austenite (A) into 9R monoclinic structure of  $\beta_2'$  martensite (M). The crystallographic parameters of 9R unit cell are:  $a = 0.441 \cdot 10^{-9}$  m,  $b = 0.268 \cdot 10^{-9}$  m,  $c = 1.92 \cdot 10^{-9}$  m and  $\beta = 88.4^\circ$  [5].

The crystalline structure of PET is formed under controlled cooling conditions and has triclinic unit cell with the parameters:  $a = 0.456 \cdot 10^{-9}$  m,  $b = 0.594 \cdot 10^{-9}$  m and  $c = 1.075 \cdot 10^{-9}$  m and the angles:  $\alpha = 98.5^\circ$ ,  $\beta = 118^\circ$  and  $\gamma = 112^\circ$  [6].

The properties of both CuZnAl SMA and PET depend upon their actual condition. The former can be in austenitic or martensitic state while the latter can be amorphous or crystalline and, in addition, its properties depend on both time and temperature. CuZnAl SMA and crystalline PET have rather close mechanical characteristics. Thus, tensile strength is 700-800 MPa at CuZnAl and 45-145 MPa at PET; elongation to failure is 10-15% and 11-35% and tensile elasticity modulus is 70 GPa and 2.3-10.3 GPa, respectively [7, 8].

In order to develop reproducible strokes, SMAs must experience a reversible martensitic transformation. In martensitic state, the material is deformed into the so-called “cold shape” and its microstructure comprises mostly stress induced martensite [9]. During heating, the microstructure retransforms, from stress induced martensite to austenite, and the macroscopic “hot shape” is instantly recovered, in the same time with the microstructure, by free-recovery shape memory effect (SME). Thermoelastic martensite is softer than austenite and the SMA is able to develop work-generating SME. After a number of cooling-deformation-heating cycles, in the framework of a thermomechanical treatment called training, the SMA is able to instantly recover its hot and cold shapes during heating and cooling, respectively, by two-way shape memory effect (TWSME) [10, 11].

---

\* email: dianalacatusu@yahoo.com, Phone: 0726261018

The principle of obtaining SME in SMPs depends on the particularities of the conditioning / programming treatment. After loading, the polymer is cooled in deformed condition and its shape is “frozen” since some polymeric chains become crystallized, therefore rigid and act as crosslink points. So, the elongated (temporary) shape is kept after unloading. In the final step, during heating, the micro-crystals melt and stored stresses contribute to the recovery of permanent shape. The origin of SME in polymers consists in the superior stiffness of micro-crystal parts, which are formed during the cooling process and become flexible during heating [12].

The present paper aims to comparatively analyse the thermodynamic and work-generating behaviours of a CuZnAl SMA and a multilayer PET heat-shrinkable sheath.

## Experimental part

Martensitic specimens, with chemical composition Cu-14.86 Zn-5.81 Al (mass. %) were hot-rolled and prepared, according to the procedure detailed in [13], for differential scanning calorimetry (DSC) analysis and bending work-generating SME experiments.

The former used specimens lighter than 50 mg, cut with a BUEHLER low speed saw and analysed by means of a 2920 Modulated DSC TA INSTRUMENTS unit, with measuring accuracies of  $\pm 0.1$  K for temperature and  $\pm 1$  W/kg for heat flow, equipped with professional software. The specimens were heated and cooled with 10 K/min, under He + Ar protective atmosphere [14].

Work-generating SME experiments used 0.5 by 4 by 50 mm lamellar CuZnAl SMA specimens which were trained in bending according to the procedure illustrated in figure 1.

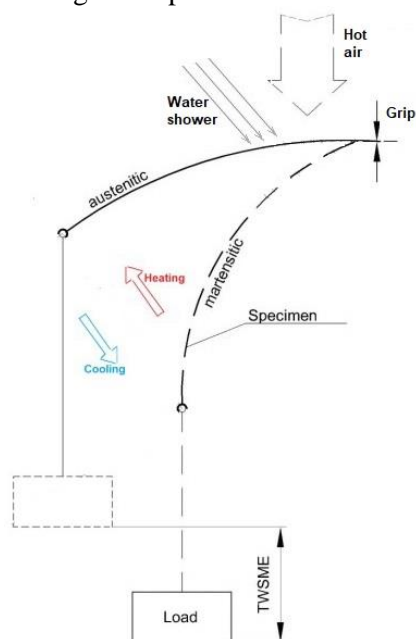


Fig. 1. Illustration of the training procedure applied to CuZnAl to develop TWSME



Fig. 2. Experimental setup for determining work-generating SME developed by ring- shaped specimens cut from heat-shrinkable polymeric sheaths

Being martensitic at room temperature, the specimens (weighing 1.7 g) were bent by the applied load (788 g). During heating, they became austenitic and lifted the load by simple SME. During cooling, the specimens became martensitic again (*i.e.* softer) and lowered the load. During the experiments cinematographic analysis enabled to determine the vertical displacement position of specimen's free end corresponding to each temperature value, determined with a multimeter's thermocouple fixed under the specimen, in the bending zone [15].

A commercial three-layer heat-shrinkable PET sheath was used for DSC and work-generating experiments. The former were performed on a NETZSCH differential scanning calorimeter type DSC 200 F3 Maya, with sensitivity:  $<1.0$  W, temperature accuracy of 0.1 K and enthalpy accuracy-generally  $<1.0\%$ . The device was calibrated with Bi, In, Sn, and Zn standards as required by DSC tests performed on polymers [16]. The latter employed a special experimental setup illustrated in figure 2.

In principle, the ring-shaped specimen, weighing approx. 0.7 g, was cut from three-layer PET heat shrinkable sheath and fastened at one end in a grip, solidary with the resistance frame, while the other end is elongated by the system formed by the inextensible thread-pulley-load. An insulated electrical resistance heats up the siliconic oil, thus triggering the shrinkage of PET ring specimen. During shrinkage, the ring lifts the load. In this case, again, cinematographic analysis enables to associate temperature values (determined with the same multimeter's thermocouple fixed under the specimen) with successive vertical positions of the load. The experiment was repeated three times, on three different specimens, under the effect of three loads: 270, 590 and 1100 g, respectively.

## Results and discussions

### DSC experiments

The typical DSC thermogram, recorded with a 25.6 mg fragment cut from CuZnAl lamellar specimen, is shown in figure 3.

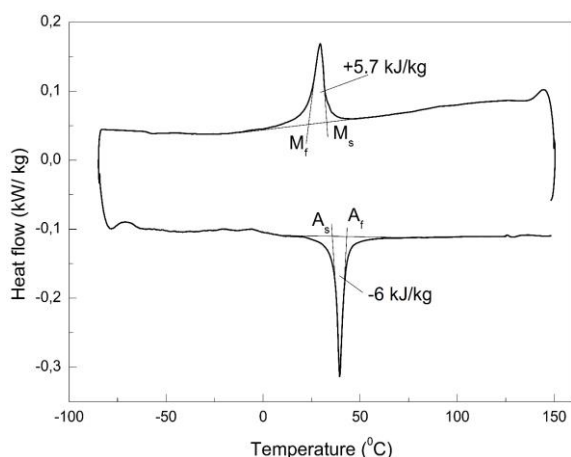


Fig. 3. Typical DSC thermogram of a fragment of CuZnAl specimen, recorded during a cooling-heating cycle.

The thermal cycle started at 150°C, where it was demonstrated that the specimen was fully austenitic [17]. During controlled cooling, direct/ forward martensitic transformation is produced, between  $M_s$  and  $M_f$ , being associated with the heat flow exothermic maximum. Since the transformation is reversible, the heat flow endothermic minimum, occurring during heating, can be ascribed to the reverse martensitic transformation, to austenite, between the critical temperatures  $A_s$  and  $A_f$ . Direct martensitic transformation released a specific enthalpy of  $h_{CuZnAl}^{cooling} = +5.7 \text{ KJ/Kg}$  while reverse transformation absorbed  $h_{CuZnAl}^{heating} = -6 \text{ KJ/Kg}$ , in good agreement with the results found in literature [13].

The DSC thermogram recorded during the heating to 180°C of a 20 mg-fragment cut from a three-layer heat-shrinkable PET sheath is shown in figure 4.

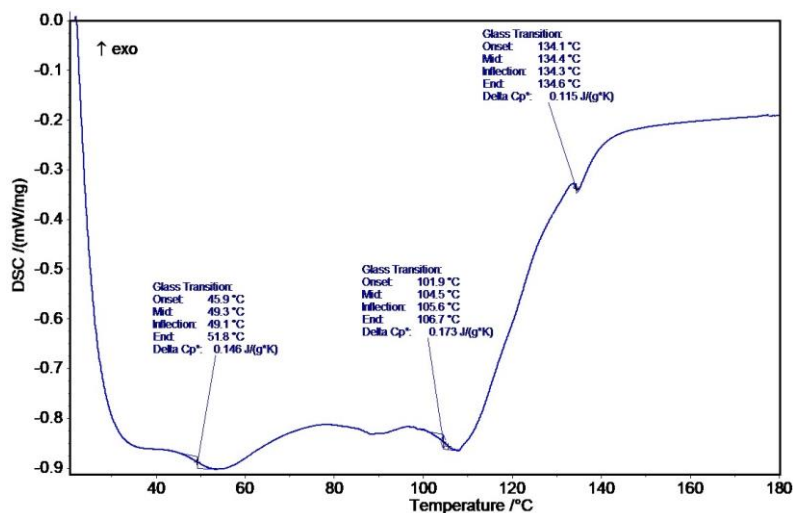


Fig. 4. DSC thermogram recorded during heating of a fragment cut from PET heat-shrinkable sheath, experiencing three glass transitions

It is noticeable that up to three glass transitions can be identified, corresponding to the number of layers. The three glass transitions occurred between: (i) 45.9 and 51.8°C (with midpoint at 49.3°C); (ii) 101.9 and 106.7°C (with midpoint at 104.5°C) and (iii) 134.1 and 134.6°C (with midpoint at 134.4°C). They were accompanied by specific heat variations of 0.146, 0.173 and 0.115 kJ/(kg×K). These results suggest that heat-shrinkage became more and more effective with temperature increasing, in such a way that additional layers got involved in the process. It is obvious that crystalline PET cannot store as much energy as a CuZnAl SMA does.

### Work-generating SME

The work-generating experiments on CuZnAl comprised repetitive heating-cooling cycles applied by means of a hot-air gun and a water sprayer, respectively, while monitoring vertical position of specimen's free end and specimen's temperature. Figure 5 summarizes the main results.

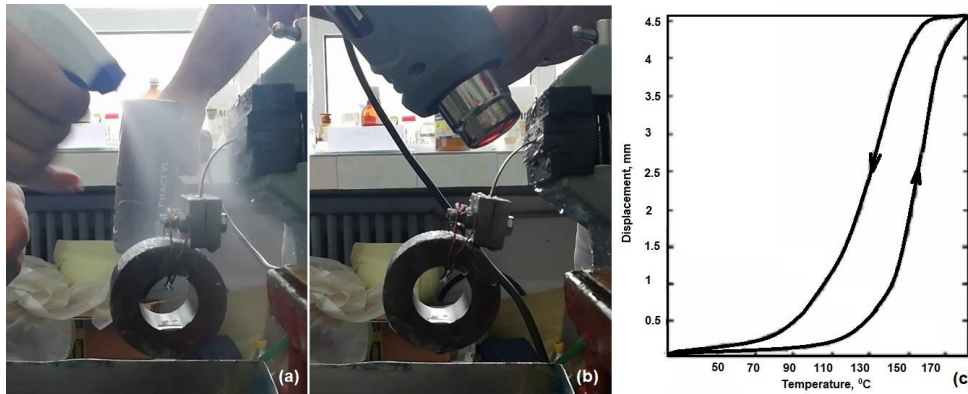


Fig. 5. Summary of work-generating experiments performed on lamellar specimen CuZnAl SMA weighing 1.7 g and lifting a 788 g load, during 20 heating-cooling cycles: (a) cold shape, at the end of cooling in the 20th cycle; (b) hot shape at the end of heating in the 20th cycle; (c) free end displacement-temperature variation during the 20th heating-cooling cycle

Figure 5a shows the specimen's shape at the end of the 20<sup>th</sup> cycle. Obviously, as an effect of both cooling-induced softening and bending caused by applied load (which is more than 460 times heavier) the specimen's free end became almost vertical. At the end of the heating stage, figure 5b illustrates an obvious lifting of the load, with approximately 4.8 mm. Finally, figure 5c displays the variation of free end's displacement as a function of temperature. In this case, generated work has been:

$$W_{CuZnAl} = 0.788kg \times 0.0048m = 3.7824 \times 10^{-3}J \quad (1)$$

and the specific work output is given by:

$$w_{CuZnAl} = 3.7824 \times 10^{-3}J/1.7 \times 10^{-3}kg \approx 2.225 J/kg \quad (2)$$

By comparing the values of released and absorbed enthalpies ( $h_{CuZnAl}^{cooling} = +5.7 KJ/Kg$  and  $h_{CuZnAl}^{heating} = -6 KJ/Kg$ , respectively) with that of specific work output,  $w_{CuZnAl} = 2.225 J/kg$ , the work-generating capacity of the CuZnAl SMA under study can be determined as:

$$W_{CuZnAl}^{Cap.} = h_{CuZnAl}^{heating} / w_{CuZnAl} \approx 2697 \quad (3)$$

This proves that only a very small part ( $3.7 \times 10^{-4}$ ) of CuZnAl SMA's energy storage capacity was used for work-generating SME, even if the load was over 463 times heavier than the specimen.

The initial and final positions of the applied loads, during the three work-generating experiments performed on three ring-shaped specimens cut from three-layer PET heat shrinkable sheath, are illustrated in figure 6.



Fig. 6. Load-lifting by work-generating SME performed by a ring shaped specimen (0.7 g) cut from a multi-layered PET heat-shrinkable sheath: (a) for a 270 g load; (b) for a 590 g load and (c) for a 1100 g load

It is obvious that the lighter the load the higher the lifting distance. Considering the three glass transitions observed in figure 4, it is obvious that only the first one located at 49.3°C took place and the second one, located around 104.5°C

and was only initiated.

By cinematographic analysis, the variation with temperature of load's vertical displacement, as an effect of PET's heat shrinkage, were plotted in figure 7.

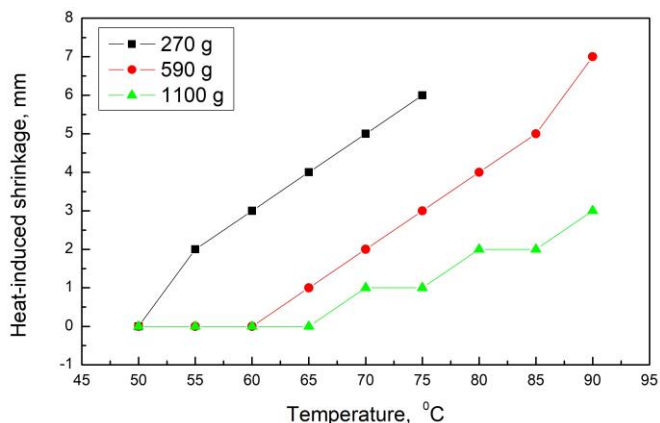


Fig. 7. Load influence on the variation with temperature of heat-induced shrinkage of PET ring-shaped specimens

Considering the heaviest load, 1.1 kg and the total lifting distance of 3 mm, the generated work is:

$$W_{PET} = 1.1kg \times 0.003m = 3.3 \times 10^{-3}J \quad (4)$$

Since specimen's mass is 0.7 g, it follows that specific work output is:

$$w_{PET} = 3.3 \times 10^{-3} \times J/0.7 \times 10^{-3}kg \approx 4.714 J/kg \quad (5)$$

If we consider the enthalpy variation of the first glass transition, by multiplying its specific heat variation 0.146 kJ/(kg×K) with the total thermal range (between 45.9 and 51.8°C) and the enthalpy variation of the second glass transition, occurring between 101.9°C and the maximum temperature reached during heating (104°C), while considering the its specific heat variation of 0.173 kJ/(kg×K), it follows that total enthalpy variation, during heating up to 140°C, is:

$$h_{PET} = [(51.8 - 45.9)K \times 0.146KJ/(Kg \times K)] + [(104 - 101.9)K \times 0.173KJ/(Kg \times K)] \approx 1.225 KJ/Kg \quad (6)$$

By comparing total enthalpy variation during heating with specific work output, it follows that the work-generating capacity of PET three-layer heat-shrinkable sheath, under study is:

$$W_{CuZnAl}^{Cap.} = h_{PET}/w_{PET} \approx 260 \quad (7)$$

This ratio shows that, in spite of the fact that it uses only a small part of its energy storage capacity ( $3.8 \times 10^{-3}$ ) for work-generating SME, the ring-shaped specimen of PET heat-shrinkable sheath is however ten times more effective as compared to CuZnAl SMA, in the conditions that it lifts a load which is over 1571 times heavier.

## Conclusions

In the case of two different shape memory materials, a Cu-14.86 Zn-5.81 Al (mass %) SMA and a three-layer PET heat-shrinkable sheath, the thermodynamic behaviour and work-generating capacity were analysed, by comparing the DSC thermograms and their respective potential to develop work output.

A 25.6-mg fragment cut from CuZnAl lamellar specimen experienced a reversible martensitic transformation, between 150 and  $-70^{\circ}C$ , characterized by a specific absorbed enthalpy of 6 kJ/kg, while the entire 1.7 g specimen lifted a 788 g load over a distance of 4.8 mm, delivering a specific work output of 2.225 J/kg.

A 20 mg fragment cut from a PET three-layer heat shrinkable sheath experienced a complete and a partial glass transition, when heated to  $104^{\circ}C$ , characterized by a total specific absorbed enthalpy of 1.225 kJ/kg, while a ring-shaped specimen, weighing 0.7 g lifted a load of 1100 g over 3 mm, when heated to the same temperature, thus delivering a specific work output of 4.714 J/kg.

A direct comparison of the two thermodynamic responses enables the following conclusions to be drawn:

- only the solid state transition occurring in CuZnAl SMA has been reversible;
- during heating, CuZnAl SMA absorbed almost 4.9 times more specific enthalpy as compared to PET heat-shrinkable sheath.

A direct comparison of the two work output performances reveals the following conclusions:

- the PET specimen lifted a load 1571 times heavier while the load lifted by CuZnAl SMA specimen was only 463 times;

- the specific work output of PET (4.714 J/kg) was at least double than that of CuZnAl SMA (2.225 J/kg);
- the work-generating capacity of PET ( $3.8 \times 10^{-3}$ ) is one order of magnitude larger than that of CuZnAl SMA ( $3.7 \times 10^{-4}$ );
- CuZnAl SMA is preferred for actuators development due to its capacity to produce reversible movements.

## References

1. WILHELM, E., RICHTER, C., RAPP, B.E., *Sensors and Actuators A*, **271**, 2018, p. 303.
2. SUN, L., HUANG, W.M., DING, Z., ZHAO, Y., WANG, C.C., PURNAWALI, H., TANG, C., *Materials and Design*, **33**, 2012, p. 577.
3. VAN HUMBEECK, J., STALMANS, R., CHANDRASEKARAN, M., *Engineering Aspects of Shape Memory Alloys*, (Duerig TW, Melton KN, Stöckel D, Wayman CM, editors), Butterworth-Heinemann, London, 1990, p. 96.
4. GHERGHESCU, I.A., JICMON, G.I., COTRUT, C., BRANZEI, M., BERBECARU, A.C., PREDESCU, A.M., CIUCA, S., *Rev. Chim. (Bucharest)*, **67**, no. 9, 2016, p. 1734-1738.
5. HARRISON, J.D., *Engineering Aspects of Shape Memory Alloys*, (Duerig TW, Melton KN, Stöckel D, Wayman CM, editors), Butterworth-Heinemann, London, 1990, p. 106.
6. LIEBERMAN, D.S., SCHMERLING, M.A., KARZ, R.W., *Shape Memory Effects in Alloys*, (Perkins J, editor), Plenum Press, New York, 1975, p. 203.
7. BUJOREANU, L.G., MUNTEANU, C., IONITA, I., TEMNEANU, M., KOGANICEANU, V. *Bulletin of the Polytechnic Institute of Iasi, LI(LV)*, **4**, *Material Science and Engineering*, 2005, p. 43.
8. EARAR, K., MATEI, M., MARECI, D., TRINCA, L.C., ARITON, M.A., AROTARITEI, D., CERGHIZAN, D., BICA, C., *Mat. Plast.*, **53**, no. 3, 2016, p. 550.
9. GHERGHESCU, I.A., TARCOLEA, M., JICMON, G.L., TURCAS, C.V., *Rev. Chim. (Bucharest)*, **64**, no. 4, 2013, p. 407-413.
10. BUJOREANU, L.G., STANCIU, S., ENACHE A., LOHAN, C., RUSU, I., *Journal of Optoelectronics and Advanced Materials*, **10**, no. 3, 2008, p. 602.
11. GRADINARU, I., TIMOFTE, D., VASINCU, D., TELSOIANU, D., CIMPOESU, R., MANOLE, V., GHEUCA-SOLOVASTRU, L., *Mat. Plast.*, **51**, no. 3, 2014, p. 230.
12. FARZANEH, S., FITOUSSI, J., LUCAS, A., BOCQUET, M., TCHARKHTCHI, A., *Journal of Applied Polymer Science*, **128**, no. 5, 2013, p. 3240, DOI: 10.1002/, 2012, app.38530.
13. BUJOREANU, L.G., *Materials Science and Engineering A*, **481-482**, 2008, p. 395.
14. BUJOREANU, L.G., LOHAN, N.M., PRICOP, B., CIMPOEȘU, N., *Journal of Materials Engineering and Performance*, **20**, no. 3, 2011, p. 468.
15. BUJOREANU, L.G., *Journal of Optoelectronics and Advanced Materials*, **17**, no. 9-10, 2015, p. 1437.
16. CIUBOTARIU, A.P., MICU, C.A., LOHAN, N.M., PRICOP, B., BUJOREANU, L.G., BEJINARIU, C., *IOP Conference Series: Materials Science and Engineering*, **374**, 2018, p. 012.
17. BUJOREANU, L.G., CRAUS, M.L., STANCIU, S., DIA, V., *Materials Science and Technology*, **16**, 2000, p. 612.

---

Manuscript received: 29.11.2019